

On-line Configuration-optimizing Control of Redundant Manipulator Based on AMSIP

Yusaku Nakamura¹, Tongxiao Zhang¹ and Mamoru Minami²

¹Graduate school of Engineering, University of Fukui, Bunkyo3-9-1, Fukui, Japan
(Tel : +81-776-27-8527; Email: {yuusaku,zhangtongxiao}@rc.his.fukui-u.ac.jp)

²Faculty of Engineering, University of Fukui, Bunkyo3-9-1, Fukui, Japan
(Tel,Fax: +81-776-27-8527; E-mail: minami@rc.his.fukui-u.ac.jp)

Abstract: This paper is concerned with real-time trajectory tracking and obstacle avoidance control using the avoidance manipulability of redundant manipulators. We had proposed a new index to evaluate the shape-changing ability in the configuration space while the manipulator's hand tracks a desired trajectory. Using this index we construct a new real-time configuration control system with the preview evaluation by introducing an imaginary manipulator at future time. The proposed system has been evaluated by several simulations and real experiments on the view points of real-time configuration optimization and feasibilities of the whole control system.

Keywords: Redundant manipulators, avoidance manipulability, preview control, 1-step GA, PA10.

1. INTRODUCTION

Kinematically redundant manipulators have more Degrees of Freedom (DoF) than necessary for accomplishing a given task. Nowadays, redundant manipulators are used for various kinds of tasks, for example, welding, sealing, grinding and contact tasks. These kinds of tasks require the manipulator to plan its hand onto the desired trajectory and avoid its intermediate links from obstacles existing near the target object and also the target object itself. Based on this purpose, in this paper we construct a system shown in Fig.1 which is able to operate any working object of whatever shape without any preparation.

There are many researches on motion and obstacle avoidance of redundant manipulators discussing how to use the redundancy. The proposed solutions to these problems can be basically categorized as Global Methods and Local Methods. In Global Methods, a method using potential function was presented [1]. Factor-Guided algorithm that finds plans of motion from one arm configuration to a goal arm configuration in 2D space was presented [2]. In [3], Ahuactzin and Gupta proposed a global method (Kinematic Roadmap) to find a series of reachable configurations (a feasible path) from a given initial configuration to goal position based on a concept called "reachability". Moreover, Global Methods are computationally very expensive, and the computational cost increases rapidly as a function of the number of manipulator joints. Therefore, considering these limitations, Global Methods are implemented only as an off-line path/motion planning tool in the high level of the manipulator control hierarchy. On the other hand, to achieve the ability to adapt for dynamic environment, the system must make every effort to be adaptable even in an environment with limited information. This adaptability requires that the system be flexible for the changing environment and could be realized with a real-time measurement ability. Such methodologies are called Local Methods. Various approaches of the real-time obstacle avoidance for redundant manipulators were presented

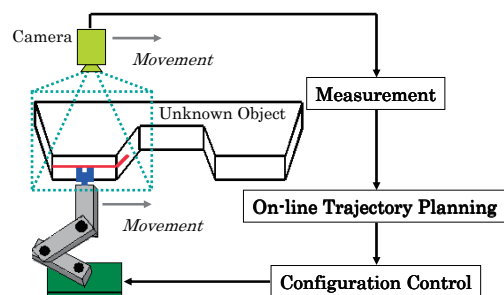


Fig. 1 Processing System for Unknown Object

[4],[5]. Real-time singular configurations avoidance was presented [6]. In general, Local Methods are mainly used to deal with moving obstacles in an unstructured dynamic environment.

Up to now, the manipulability ellipsoid[7] was presented to evaluate the static performance of a robot manipulator as an index of the relationship between the angular velocities at each joint and the linear velocity at the end-effector of the manipulator. Also, the manipulability measure was addressed for cooperative arms [8]. Especially, the manipulability measure was used in real-time control [9]. However, the manipulability ellipsoid is just based on kinematics; the manipulator dynamics are completely ignored. The manipulating force ellipsoid [10] was presented to evaluate the static torque-force transmission from the joints to the end-effector, while the dynamic manipulability ellipsoid [11] was presented as an index of the dynamic performance of a robot manipulator based on the maximum acceleration of the end-effector. Combining the manipulating force ellipsoid with the dynamic manipulability, the inertia matching ellipsoid [12] was proposed to characterize the dynamic torque-force transmission efficiency.

Our research just pursues the adaptable system categorized in Local Method. Fig.1 shows an on-line shape detection/processing system. In Fig.1, the camera and the manipulator's hand are supposed to move synchronously

to achieve an on-line adaptive operation depending on the real-time information of limited known environment (the changing shape and position of target object) obtained by this moving camera. The unknown environment outside the range of the camera changes as the process progresses. The range area of the camera is limited and the size of the target object is not limited, so it is reasonable to assume that the camera range is smaller than the object size. Then, once there appears an obstacle suddenly in the scene of camera, the manipulator must change its shape as quickly as possible so that it can avoid this obstacle. In addition, Local Methods have such merits as less computation and real-time adaptability. This requires the manipulator possess the ability to avoid this moving obstacle suddenly appearing in the limited camera range by changing its shape quickly. Therefore, it is very necessary and meaningful to keep the optimal shape-changing ability of the redundant manipulator in the whole on-line working process (trajectory tracking and obstacle avoidance).

The manipulability ellipsoid had been proposed to evaluate the easiness of the end-effector of the manipulator arbitrarily changing its position and orientation. The avoidance manipulability concept [13] was derived inspired from the manipulability ellipsoid and was firstly presented in our previous research, which just was used to evaluate the shape-changing ability of each intermediate link except the end-effector. However, in [13], the avoidance manipulability ellipsoid just evaluated the shape-changing ability of each intermediate link but did not evaluate the avoidance manipulability of the whole manipulator.

Therefore, firstly, we introduce an index to evaluate the avoidance manipulability of the whole manipulator by defining the sum of volume of each avoidance manipulability ellipsoid corresponding to each intermediate link, which is called "AMSI"(Avoidance Manipulability Shape Index) [14]. Then, considering the potential spaces along the target object's shape along with the AMSI, we propose another new index called "AMSIP"(Avoidance Manipulability Shape Index with Potential). Finally, using "AMSIP" combining with 1-Step Genetic Algorithm (GA) [15] to solve the on-line optimization problem of multi-peak and time-varying AMSIP distribution, we realize a new processing system with optimized adaptability for avoidance ability while its hand tracks the desired trajectory on the object with limited information with the target's shape.

2. AVOIDANCE MANIPULABILITY

Representing the vector of position and orientation of each link by $\mathbf{r}_i \in R^m (i = 1, 2, \dots, n)$ where m denotes the dimension of working space, n denotes the number of links of manipulator. Representing the vector of joint angles by $\mathbf{q} = [q_1, q_2, \dots, q_n]^T$. \mathbf{r}_i is given by (1) as a function of \mathbf{q} .

$$\mathbf{r}_i = \mathbf{f}_i(\mathbf{q}), (i = 1, 2, \dots, n) \quad (1)$$

By differentiating (1) by time t , we can obtain (2).

$$\dot{\mathbf{r}}_i = \mathbf{J}_i(\mathbf{q})\dot{\mathbf{q}} \quad (2)$$

In (2), $\mathbf{J}_i(\mathbf{q}) \in R^{m \times n}$ is Jacobian matrix differentiated \mathbf{r}_i by \mathbf{q} . Here we discuss the case that desired trajectory \mathbf{r}_{nd} and desired velocity of the manipulator's hand $\dot{\mathbf{r}}_{nd}$ are given as primary task. Then, according to (2) we can obtain $\dot{\mathbf{q}}$ realized by $\dot{\mathbf{r}}_{nd}$.

$$\dot{\mathbf{q}} = \mathbf{J}_n^+ \dot{\mathbf{r}}_{nd} + (\mathbf{I}_n - \mathbf{J}_n^+ \mathbf{J}_n) {}^1\mathbf{l} \quad (3)$$

where \mathbf{J}_n is Jacobian matrix differentiated \mathbf{r}_n by \mathbf{q} , \mathbf{J}_n^+ is pseudo-inverse of \mathbf{J}_n , \mathbf{I}_n is $n \times n$ unit matrix, and ${}^1\mathbf{l}$ is an arbitrary vector satisfying ${}^1\mathbf{l} \in R^n$. The left superscript "1" of ${}^1\mathbf{l}$ means the first sub-task executed by using redundant degrees of freedom. If the rest redundant degrees of freedom can execute another sub-task besides the first sub-task, we define it by ${}^2\mathbf{l}$, which indicate the avoidance action in higher dimension [13]. The following definitions about left superscript "1" are also. In the right side of (3), the first term is the solution to make $\|\dot{\mathbf{q}}\|$ minimize in the space of $\dot{\mathbf{q}}$ while realizing $\dot{\mathbf{r}}_{nd}$. The second term is joint angle velocity component that can change the manipulator's configuration regardless with the influence of $\dot{\mathbf{r}}_{nd}$. When the first avoidance sub-task is given to the i -th link, in other words, the first demanded velocity ${}^1\dot{\mathbf{r}}_{di}$ is determined by an avoidance control system of higher level depending on geometric relation of a manipulator with an obstacle. The relation of ${}^1\dot{\mathbf{r}}_{di}$ and $\dot{\mathbf{r}}_{nd}$ is shown in (4) by substituting (3) into (2).

$${}^1\dot{\mathbf{r}}_{di} = \mathbf{J}_i \mathbf{J}_n^+ \dot{\mathbf{r}}_{nd} + \mathbf{J}_i (\mathbf{I}_n - \mathbf{J}_n^+ \mathbf{J}_n) {}^1\mathbf{l} \quad (4)$$

Here we define two variables shown in (5) and (6).

$$\Delta^1\dot{\mathbf{r}}_{di} \triangleq {}^1\dot{\mathbf{r}}_{di} - \mathbf{J}_i \mathbf{J}_n^+ \dot{\mathbf{r}}_{nd} \quad (5)$$

$${}^1\mathbf{M}_i \triangleq \mathbf{J}_i (\mathbf{I}_n - \mathbf{J}_n^+ \mathbf{J}_n) \quad (6)$$

According to (5) and (6), $\Delta^1\dot{\mathbf{r}}_{di}$ can be rewritten by (7).

$$\Delta^1\dot{\mathbf{r}}_{di} = {}^1\mathbf{M}_i {}^1\mathbf{l} \quad (7)$$

In (7), $\Delta^1\dot{\mathbf{r}}_{di}$ is represented by the first avoidance velocity and ${}^1\mathbf{M}_i$ is a $R^{m \times n}$ matrix represented by the first avoidance matrix.

Next, we will represent the avoidance manipulability measure and the avoidance manipulability ellipsoid. Providing that ${}^1\mathbf{l}$ is restricted as $\|{}^1\mathbf{l}\| \leq 1$, then the extent where $\Delta^1\dot{\mathbf{r}}_{di}$ can move is denoted by (8).

$$\Delta^1\dot{\mathbf{r}}_{di}^T ({}^1\mathbf{M}_i^+)^T {}^1\mathbf{M}_i^+ \Delta^1\dot{\mathbf{r}}_{di} \leq 1 \quad (8)$$

If $\text{rank}({}^1\mathbf{M}_i) = m$, the ellipsoid represented by (8) is named as the first complete avoidance manipulability ellipsoid. If $\text{rank}({}^1\mathbf{M}_i) = p < m$, the ellipsoid is named as the first partial avoidance manipulability ellipsoid.

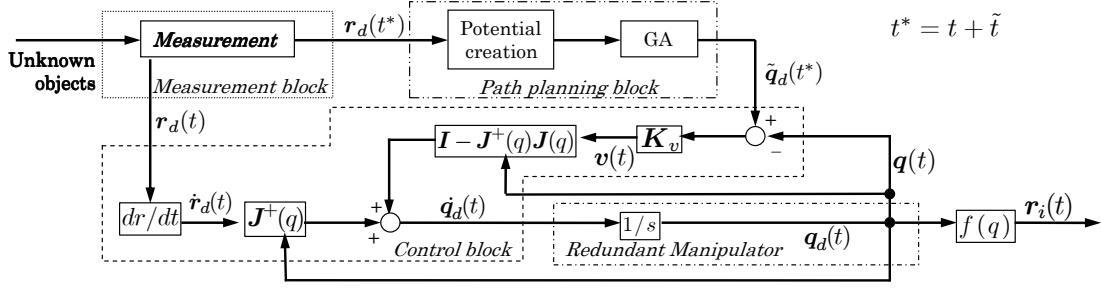


Fig. 2 Preview Control System

3. PREVIEW CONTROL SYSTEM

Preview control system is a configuration control method, which is shown in Fig.2. t denotes the current time, t^* denotes the future time and t^* is forwarder than t by \tilde{t} ($\tilde{t} = t^* - t$). Here, \tilde{t} is called “preview time”. Preview control system consists of a real-time measurement block, a planning block, a redundancy control block and a redundant manipulator. Firstly, the measurement block can detect the desired hand position $r_d(t^*)$ on the surface of working object (target object) at future time t^* . Next, the planning block outputs the future joint angles $\tilde{q}_d(t^*)$ satisfying non-collision corresponding to the future desired hand position $r_d(t^*)$ (at future time t^*) referring to potential spaces. This is called “imaginary manipulator”.

Here, we need to introduce the potential spaces, which are detected by camera and are created around the working object’s shape automatically at the planning block. As shown in Fig.3, the potential spaces u_k ($k = 0, 1, 2, \dots, n_k$) are set along the working object’s shape with the interval of Δh , here n_k denotes the number of potential spaces. And the potential values v_k ($k = 0, 1, 2, 3, \dots, n_k$) denote the dangerous extent, which are defined by $v_0 < v_1 < v_2 < \dots < v_{n_k} < 0$. That is to say, if the distance with the working object becomes nearer, the potential value will become smaller. In addition, the specified points are placed on each link of the manipulator, and the coordinates of the specified points are represented by $s_{ij}(x_{ij}, y_{ij})$ [$i = 1, 2, 3, \dots, n; j = 1, 2, \dots, n_i$] where n denotes the number of manipulator’s links and n_i denotes the sum number of the specified points in i -th link. Evaluation value $a(s_{ij})$ of specified point s_{ij} is defined by (9).

$$\begin{cases} a(s_{ij}) = v_k & s_{ij} \in u_k \\ a(s_{ij}) = 0 & \text{otherwise} \end{cases} \quad (9)$$

Total potential value U of the imaginary manipulator’s shape at future time t^* is defined by (10).

$$U = \sum_{i=1}^n \sum_{j=1}^{n_i} a(s_{ij}) \quad (10)$$

At last, according to (11), the control block outputs the desired joint angular velocity $\dot{q}_d(t)$ that is required to make the current shape of actual manipulator $q(t)$ close the future optimal shape of imaginary manipulator $\tilde{q}_d(t^*)$ with the optimal shape-changing ability based on non-collision when the desired velocity of the manipulator’s hand $\dot{r}_d(t)$ is given.

$$\dot{q}_d(t) = J_n^+(q)\dot{r}_d(t) + [I_n - J_n^+(q)J_n(q)]v(t) \quad (11)$$

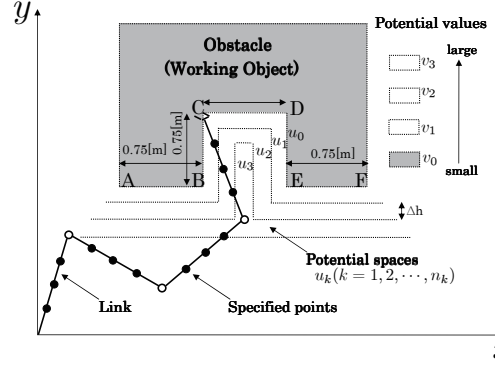


Fig. 3 Potential Spaces and Desired Hand Trajectory

where, $v(t)$ is an important arbitrary vector satisfying $v(t) \in R^n$ through which trajectory tracking and obstacle avoidance can be executed simultaneously using redundancy. In this paper, $v(t)$ is determined to make the current shape of actual manipulator $q(t)$ close the future optimal shape of imaginary manipulator $\tilde{q}_d(t^*)$, so it is defined by (12).

$$v(t) = K_v[\tilde{q}_d(t^*) - q(t)] \quad (12)$$

where, K_v is a positive definite diagonal matrix representing gains, that is, $K_v = \text{diag}[k_{v1}, k_{v2}, \dots, k_{vn}]$. Here, please notice that the future optimal shape of imaginary manipulator $\tilde{q}_d(t^*)$ used to control the current shape of actual manipulator is the really optimal shape, which possesses the better avoidance manipulability of the whole manipulator based on non-collision. The evaluation of avoidance manipulability of the whole manipulator will be introduced in next section.

4. AVOIDANCE MANIPULABILITY SHAPE INDEX (AMSI)

Here, we will present the avoidance manipulability shape index (AMSI) expressed by sum shape-changing ability of all intermediate links. The shape-changing ability of intermediate link can be evaluated by avoidance manipulability ellipsoid. The volume of avoidance manipulability ellipsoid will determine the extent of shape-changing ability. When the volume of avoidance manipulability ellipsoid of i -th link is the largest, the shape-changing ability of i -th link is the best. The volume of avoidance manipulability ellipsoid (1P_i) of i -th link is defined by (13).

$${}^1V_i = c_m \cdot {}^1w_i \quad (13)$$

where, m denotes the dimension number, c_m and 1w_i are defined by (14) and (15) respectively.

$$c_m = \begin{cases} \frac{2(2\pi)^{(m-1)/2}}{1 \cdot 3 \cdots (m-2)m} & (m : \text{odd}) \\ \frac{(2\pi)^{m/2}}{2 \cdot 4 \cdots (m-2)m} & (m : \text{even}) \end{cases} \quad (14)$$

$${}^1w_i = {}^1\sigma_{i1} {}^1\sigma_{i2} \cdots {}^1\sigma_{im} \quad (15)$$

In (15), ${}^1\sigma_{i1}, \dots, {}^1\sigma_{im}$ are the singular values of 1M_i .

The largest 1V_i corresponds to the best avoidance manipulability of i -th link. However, each 1V_i just denotes the extent of avoidance manipulability of each intermediate link. For evaluating the avoidance manipulability of the whole manipulator, AMSI (Avoidance Manipulability Shape Index) 1E is defined by (16).

$${}^1E = \sum_{i=1}^{n-1} {}^1V_i a_i \quad (16)$$

where, a_i is defined by (17).

$$a_1 = a_{n-1} = 1[m^{-1}], \quad a_{2,3,\dots,(n-2)} = 1[m^{-2}] \quad (17)$$

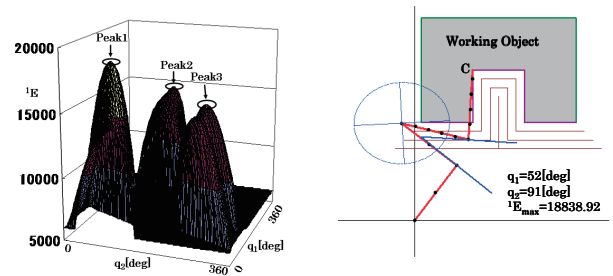
1V_1 and ${}^1V_{n-1}$ denote the length, ${}^1V_{2,3,\dots,(n-2)}$ denote square measure. By (17), 1E denotes an index without unit. In addition, if manipulator's hand can not reach the desired position, we define 1E by (18).

$${}^1E = 0 \quad (18)$$

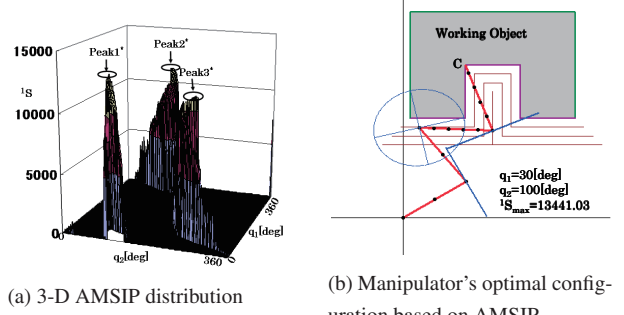
5. AVOIDANCE MANIPULABILITY SHAPE INDEX WITH POTENTIAL (AMSIP)

Although avoidance manipulability of the whole manipulator can be evaluated by using AMSI, the collision possibility is on the increase because it does not consider the distance between the manipulator and the target object. In addition, in section 3, we introduced the evaluation index using potential spaces created around the target object's shape to roughly judge the distance between the manipulator and the target object. Therefore, we define the optimal evaluation index considering avoidance manipulability and potential, which is called "Avoidance Manipulability Shape Index with Potential" (AMSIP).

$${}^1S = {}^1E + U \quad (19)$$



(a) 3-D AMSI distribution
Fig. 4 3-D AMSI distribution and manipulator's optimal configuration based on AMSI when the hand is fixed at C



(a) 3-D AMSIP distribution
Fig. 5 3-D AMSIP distribution and manipulator's optimal configuration based on AMSIP when the hand is fixed at C

Next, we will verify that AMSIP is more effective than AMSI by comparison. When the manipulator's hand moves to position C in Fig.4(b), the distribution of AMSI about q_1 and q_2 is shown in Fig.4(a), and the distribution of AMSIP is shown in Fig.5(a), where q_1 and q_2 are joint angles of link1 and link2 respectively and they constitute redundancy space of joint angles, q_3 and q_4 are determined depending on the hand position once q_1 and q_2 are confirmed. Comparing Fig.4(a) with Fig.5(a), the obvious difference can be found that the shapes of $Peak^*$ of 1S are smaller and thinner than the shapes of $Peak$ of 1E , moreover there are lots of area corresponding to ${}^1S < 0$ in AMSIP distribution. This fact just indicates that AMSIP depending on the area of ${}^1S < 0$ can avoid the collision successfully. According to Fig.4(b) and Fig.5(b), which denote the manipulator's optimal configurations corresponding to $Peak1$ and $Peak1^*$ respectively, we can find that AMSIP can avoid collision with higher avoidance manipulability. Therefore, we verify that AMSIP is more effective than AMSI.

6. TRAJECTORY TRACKING CONTROL BASED ON AMSIP

6.1 Real-time Optimization Using 1-step GA

The desired hand trajectory is shown in Fig.3, where, the surface of target object is structured by a concave from A to F. How to search on-line the changing optimal shape $\tilde{q}_d(t^*)$ is a key problem. Among the many solutions, 1-step GA is used to realize real-time optimization (searching $\tilde{q}_d(t^*)$) instead of traditional Conjugate Gradient method. In next subsection, we introduce 1-step GA.

6.2 1-step GA

Providing the structure of the manipulator is 4-link, $n = 4$, and the dimension of the space $m = 2$ as shown in Fig.3, the redundant degree is $n - m = 2$. Giving this redundant degree to q_1 and q_2 , the rest joint values q_3 and q_4 are determined depending on the hand task trajectory $r_d(t)$. The AMSIP value F at future time t^* can be expressed as $F(q(t^*))$ through joint values of $q(t^*) = [q_1, q_2, q_3, q_4]^T$.

The highest peak $q^{max}(t^*)$

$$q^{max}(t^*) = \{q(t) \mid \max_{q \in L} F(q(t^*))\}, \quad (20)$$

indicates the most effective configuration evaluated by AMSIP at time t^* , where L means redundant space of q_1 and q_2 .

$F(\mathbf{q}(t^*))$ is used as a fitness function in Genetic Algorithm (GA) to find \mathbf{q}^{max} through i -th gene ($i = 1, 2, \dots, p$) of j -th generation, $\mathbf{q}_{i,j}(t^*)$,

$$\mathbf{q}_j^{max}(t^*) = \{\mathbf{q}_{i,j}(t^*) \mid \max_i F(\mathbf{q}_{i,j}(t^*))\}. \quad (21)$$

Assuming the time “ t^* ” be fixed to one future time the problem to find $\mathbf{q}^{max}(t^*)$ in the AMSIP distribution through GA process can be described as

$$\mathbf{q}_j^{max}(t^*) \xrightarrow{\text{evolve}} \mathbf{q}^{max}(t^*), \quad (j \rightarrow \infty), \quad (22)$$

where the above convergence to target pose $\mathbf{q}^{max}(t^*)$ can be thought generally to be guaranteed with appropriate parameter setting of GA.

To recognize $\mathbf{q}^{max}(t^*)$ in a dynamic distribution changing by video rate, 33 [fps], the recognition system must have real-time nature, that is, $\mathbf{q}_j^{max}(t^*)$ must converge to the $\mathbf{q}^{max}(t^*)$. To give the GA process the real-time nature, the evolving process

$$\mathbf{q}_{i,j}(t^*) \xrightarrow{\text{evolve}} \mathbf{q}_{i,j+1}(t^* + \Delta t) \quad (23)$$

is executed only one time within the time interval of Δt . We named it as “1-step GA”. Should the converging speed of the model to the target in the dynamic images be faster than the moving speed $d\mathbf{q}^{max}(t^*)/dt$ of the $\mathbf{q}^{max}(t^*)$ in the dynamic distribution of $F(\mathbf{q}(t^*))$ as time t^* passing, that is,

$$\frac{\mathbf{q}_{j+1}^{max}(t^* + \Delta t) - \mathbf{q}_j^{max}(t^*)}{\Delta t} > \frac{d\mathbf{q}^{max}(t^*)}{dt}, \quad (24)$$

then the $\mathbf{q}_j^{max}(t^*)$ exists in a vicinity of $\mathbf{q}^{max}(t^*)$ regardless of the time of t^* since GA’s tracking speed of $\mathbf{q}_i^{max}(t^*)$ to $\mathbf{q}^{max}(t^*)$ is faster than the moving speed of $\mathbf{q}^{max}(t^*)$. Therefore above condition allows us the following on-line measurement condition of 1-step GA optimization can be satisfied,

$$|\mathbf{q}^{max}(t^*) - \mathbf{q}_j^{max}(t)| < \epsilon, \quad (25)$$

where ϵ represents tolerable extent as a observing error. We have confirmed that the above time-variant optimization problem to solve $\mathbf{q}^{max}(t^*)$ maximizing $F(\mathbf{q}(t^*))$ could be solved by 1-step GA through several experiments. Here, please notice that $\mathbf{q}^{max}(t^*)$ is given to the future optimal shape of imaginary manipulator $\tilde{\mathbf{q}}_d(t^*)$ in (12).

6.3 Analysis of Shape Optimization Control

For the desired hand trajectory from A to F shown in Fig.3, the each part length of trajectory: $L_{A-B} = L_{B-C} = L_{C-D} = L_{D-E} = L_{E-F} = 75[cm]$, the coordinate of A is fixed at position $(10[cm], 140[cm])$, the length of each link of manipulator: $l_1 = l_2 = l_3 = l_4 = 100[cm]$. The velocity of trajectory tracking of manipulator’s hand is set by $7.5[cm/s]$ ($\dot{r}_d = 7.5[cm/s]$). Preview time: $\tilde{t} = 10[s]$. Firstly, when the manipulator’s hand is fixed in B, the distribution of AMSIP based on

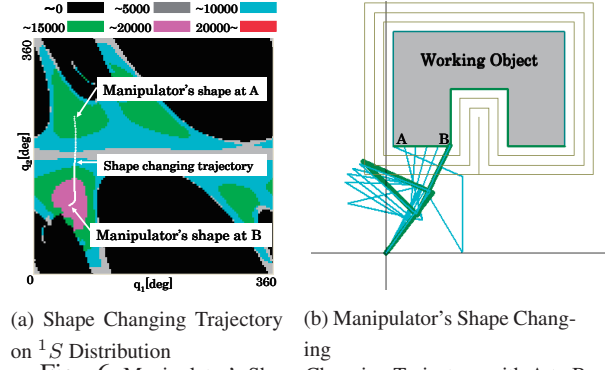


Fig. 6 Manipulator’s Shape Changing Trajectory with A to B

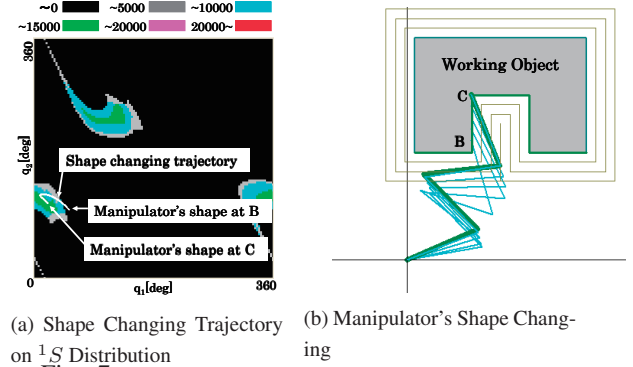


Fig. 7 Manipulator’s Shape Changing Trajectory with B to C

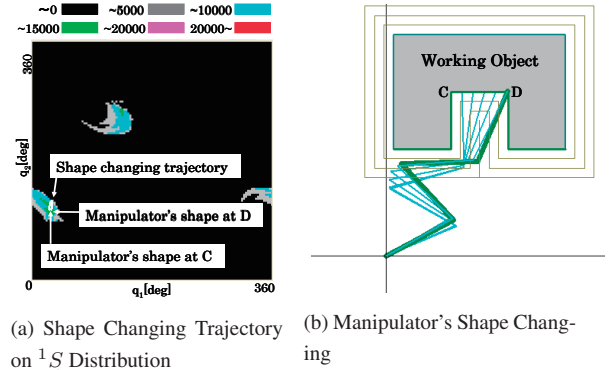
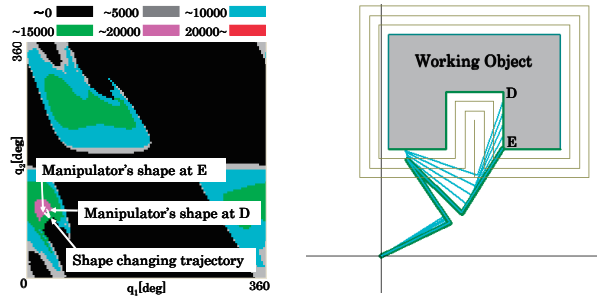


Fig. 8 Manipulator’s Shape Changing Trajectory with C to D

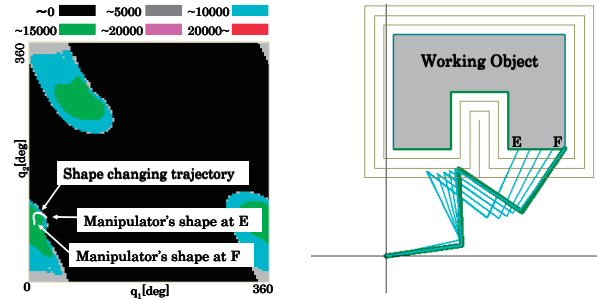
global exploration is shown in Fig.6(a). The initial shape at A can almost close the optimal shape at B. The actual manipulator’s shape changing (AMSIP changing) from A to B is shown in Fig.6(b). Similarly, when we consider the trajectory parts of B-C, C-D, D-E and E-F, the changing process of actual manipulator’s shape are shown from Fig.7 to Fig.10, respectively. According to above discussion and analysis, the effectiveness of shape optimization control of trajectory tracking based on preview control and 1-step GA is verified.

6.4 Simulations

The simulation results are shown in Fig.11. Fig.11(a) shows the really desired AMSIP of imaginary manipulator obtained by global exploration (scanning all redundant spaces), whose whole changing process along varying trajectory is described by the curve called “maximum value”. Also, Fig.11(a) shows the optimal AMSIP of imaginary manipulator obtained by 1-step GA, whose whole changing process along varying trajectory



(a) Shape Changing Trajectory on 1S Distribution
 (b) Manipulator's Shape Changing
 Fig. 9 Manipulator's Shape Changing Trajectory with D to E



(a) Shape Changing Trajectory on 1S Distribution
 (b) Manipulator's Shape Changing
 Fig. 10 Manipulator's Shape Changing Trajectory with E to F

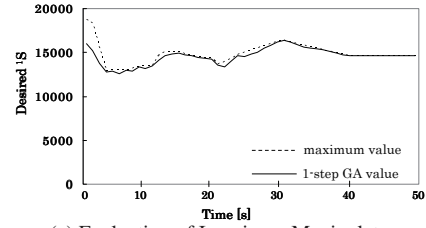
is described by the curve called “1-step GA value”. By comparing “1-step GA value” with “maximum value” in Fig.11(a), we can find that “1-step GA value” is almost coincide with “maximum value” in the whole process, we can verify feasibility of 1-step GA for real-time optimization. Fig.11(b) shows the changing process of AMSI (1E) and AMSIP (1S) of actual manipulator all the time, from which we can find the actual manipulator can keep good avoidance manipulability without collision in the whole tracking process.

7. EXPERIMENT USING PA10

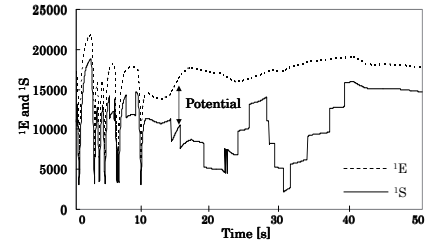
The real machine called “PA10”(Mitsubishi Heavy Industry) has 7 DoF with 7-link and can work in 3-dimension space, whose configuration is shown in Fig.12. In this section, we will use this real machine to realize real-time trajectory tracking and obstacle avoidance with higher shape-changing ability. The scenery of experient and the overview of working object is shown in Fig.scenery and Fig.overview. In this experiment, the preview time is set by $2[s]$ ($\tilde{t} = 2[s]$), the desired hand velocity is set by $5[cm/s]$ ($\tilde{r}_d = 5[cm/s]$), the desired trajectory is defined by (26).

$$\mathbf{r}_d = \begin{cases} r_{dx} = -0.7 [m] \\ r_{dy} = -0.5 + 0.05t [m] \\ r_{dz} = 0.7 [m] \end{cases} \quad (26)$$

The whole experiment (trajectory tracking and obstacle avoidance using PA10) will be finished in $20[s]$. In addition, we construct three potential spaces with $\Delta h = 10[cm]$, whose potential values are $v_1 = -10$, $v_2 = -2$ and $v_3 = -1$ respectively. The potential value inside



(a) Evaluation of Imaginary Manipulator



(b) Evaluation of Actual Manipulator

Fig. 11 Results of Real-Time Configuration Optimization

the working object is set by -10000 ($v_0 = -10000$, please notice v_0 is used to judge whether the manipulator's links avoid the working object or not). The experiment results are shown in Fig.15. From Fig.15, we can find there exists no negative value of AMSIP in the whole working process, whichever imaginary manipulator and actual manipulator, which indicates that the hand of PA10 accomplishes the whole trajectory tracking without collision. From this experiment results shown in Fig.15 using PA10, we verify the presented method can be used in the real machine successfully.

8. CONCLUSION

In this paper, a new definition “Avoidance Manipulability Shape Index”(AMSI) as an index being able to evaluate the avoidance manipulability of the whole manipulator is presented. Moreover, “Avoidance Manipulability Shape Index with Potential”(AMSIP) is presented as the optimal evaluation considering avoidance manipulability (AMSI) and potential (judging the distance between the manipulator and the target object). According to AMSIP, we can find the manipulator's optimal shape with good avoidance manipulability and non-collision. Finally, the effectiveness of real-time optimization of manipulator's shape based on AMSIP is verified by simulations and experiment using PA10.

REFERENCES

- [1] DongXiang Yang, Motoji Yamamoto, Akira Mohri “Collision-Free Trajectory Planning for Manipulator Using Potential Function”, Transactions of the Japan Society of Mechanical Engineers. C, 93-1517, pp.2345-2350 (1994).
- [2] Jaesik Choi, Eyal Amir “Factor-Guided Motion Planning for a Robot Arm”, International Conference on Intelligent Robots and Systems, pp.27-32, 2007.
- [3] Juan Manuel Ahuactzin, Kamal K. Gupta “The

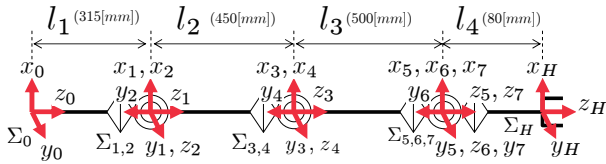


Fig. 12 Configuration of PA10

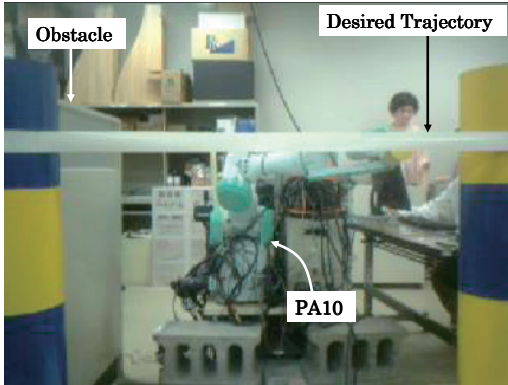


Fig. 13 Scenery of Experiment

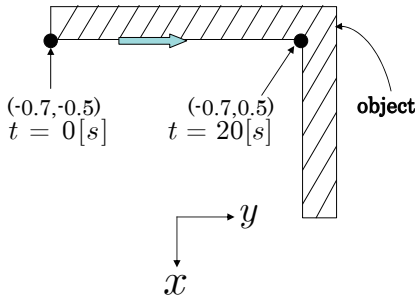


Fig. 14 Overview of Working Object

Kinematic Roadmap: A Motion Planning Based Global Approach for Inverse Kinematics of Redundant Robots”, IEEE Transactions on Robotics and Automation, Vol.15, No.4, pp.653-669, 1999.

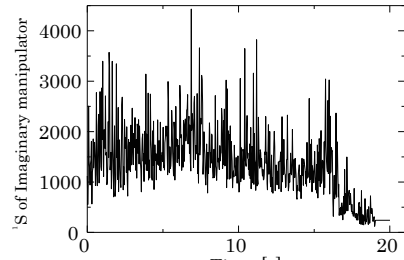
[4] Leon Zlajpah, Bojan Nemeč “Kinematic Control Algorithms for On-line Obstacle Avoidance for Redundant Manipulator”, International Conference on Intelligent Robots and Systems, pp.1898-1903, 2002.

[5] Kwang-Kyu Lee, Martin Buss “Obstacle Avoidance for Redundant Robots Using Jacobian Transpose Method”, International Conference on Intelligent Robots and Systems, pp.3509-3514, 2007.

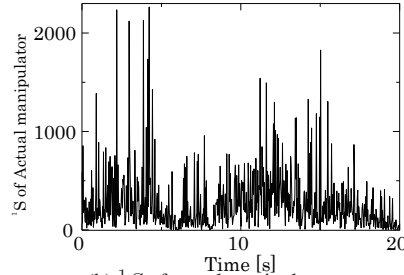
[6] Marani, G. Jinhyun Kim Junku Yuh Wan Kyun Chung, “A real-time approach for singularity avoidance in resolved motion rate control of robotic manipulator”, Proceedings of IEEE/RSJ International Conference on Robotics and Automation(ICRA), vol.2, pp.1973-1978, 2002.

[7] Tsuneo Yoshikawa “Manipulability of Robot Mechanisms”, (in Japanese) The International Journal of Robotics Research, Vol.4, No.2, pp.3-9, 1985.

[8] S. Lee “Dual Redundant Arm Configuration Optimization with Task-oriented Dual Arm Manipu-



(a) 1S of imaginary manipulator



(b) 1S of actual manipulator

Fig. 15 1S changing process

lability”, IEEE Transactions on Robotics and Automation, Vol.5, No.1, pp.78-97, 1989.

[9] Haruhisa Kawasaki, Tetsuya Mouri “Design and Control of Five-Fingered Haptic Interface Opposite to Human Hand”, IEEE Transactions on Robotics, Vol.23, No.5, pp.909-918, 2007.

[10] Ralf Koeppe, Tsuneo Yoshikawa “Dynamic Manipulability Analysis of Compliant Motion”, Proceedings of IEEE/RSJ International Conference on Intelligent Robots and Systems(IROS), vol.3, pp.1472-1478, 1997.

[11] Tsuneo Yoshikawa “Dynamic Manipulability of Robot Manipulators”, (in Japanese) Journal of Robotic Systems, Vol.2, No.1, pp.113-124, 1985.

[12] Ryo Kurazume, Tsutomu Hasegawa “A New Index of Serial-Link Manipulator Performance Combining Dynamic Manipulability and Manipulating Force Ellipsoid”, IEEE Transactions on Robotics, Vol.22, No.5, pp.1022-1028, 2006.

[13] Mamoru Minami, Yoshihiro Nomura, Toshiyuki Asakura “Avoidance Manipulability of Redundant Manipulators”, Journal of the Robotics Society of Japan, Vol.17, No.6, pp.887-895, 1999.

[14] Hiroshi Tanaka, Mamoru Minam, Yasushi Mae, “Trajectory Tracking of Redundant Manipulators Based on Avoidance Manipulability Shape Index”, Proceedings of IEEE/RSJ International Conference on Intelligent Robots and Systems(IROS), pp.1892-1897, 2005.

[15] Mamoru Minami, Hidekasu Suzuki, Julien Agbanhan “Fish Catching by Robot Using Gazing GA Visual Servoing”, Transactions of the Japan Society of Mechanical Engineers. C, Vol.68, No.668, 1198-1206 (2002).